

Plutonium interaction studies with the Mont Terri Opalinus Clay isolate Sporomusa sp. MT-2.99: changes in the plutonium speciation by solvent extractions.

Moll, H.; Cherkouk, A.; Bok, F.; Bernhard, G.;

Originally published:

April 2017

Environmental Science and Pollution Research 24(2017)15, 13497-13508

DOI: <https://doi.org/10.1007/s11356-017-8969-6>

Perma-Link to Publication Repository of HZDR:

<https://www.hzdr.de/publications/Publ-24118>

Release of the secondary publication
on the basis of the German Copyright Law § 38 Section 4.

1 **Plutonium interaction studies with the Mont Terri Opalinus Clay**
2 **isolate *Sporomusa* sp. MT-2.99: changes in the plutonium speciation by**
3 **solvent extractions**

4 **Henry Moll***, Andrea Cherkouk, Frank Bok, and Gert Bernhard

5
6 *Helmholtz-Zentrum Dresden-Rossendorf HZDR, Institute of Resource Ecology, Bautzner Landstrasse*
7 *400, 01328 Dresden, Germany*

8

9 **Abstract**

10 Since plutonium could be released from nuclear waste disposal sites, the exploration of the complex
11 interaction processes between plutonium and bacteria is necessary for an improved understanding of the
12 fate of plutonium in the vicinity of such a nuclear waste disposal site. In this basic study the interaction of
13 plutonium with cells of the bacterium, *Sporomusa* sp. MT-2.99, isolated from Mont Terri Opalinus Clay,
14 was investigated anaerobically (in 0.1 M NaClO₄) with or without adding Na-pyruvate as an electron
15 donor. The cells displayed a strong pH dependent affinity for Pu. In the absence of Na-pyruvate a strong
16 enrichment of stable Pu(V) in the supernatants was discovered, whereas Pu(IV)-polymers dominated the
17 Pu oxidation state distribution on the biomass at pH 6.1. A pH-dependent enrichment of the lower Pu
18 oxidation states (e.g. Pu(III) at pH 6.1 which is considered to be more mobile than Pu(IV) formed at pH
19 4) was observed in the presence of up to 10 mM Na-pyruvate. In all cases, the presence of bacterial cells
20 enhanced removal of Pu from solution and accelerated Pu interaction reactions, e.g. biosorption and
21 bioreduction.

22

23 **Keywords:** plutonium; bacteria; *Sporomusa* sp.; biosorption; bioreduction; solvent
24 extractions

25

* Address correspondence to Henry Moll, Institute of Resource Ecology, Helmholtz-Zentrum Dresden-Rossendorf HZDR, Bautzner Landstrasse 400, 01328 Dresden, Germany. E-mail: h.moll@hzdr.de.

26 **Introduction**

27 One potential source of actinides (An) in the environment could be the accidental release from nuclear
28 waste disposal sites. Microorganisms indigenous in potential host rocks are able to influence the
29 speciation and therefore the mobility of An and their retardation. They can as well affect the conditions in
30 a geologic repository (e.g. by gas generation or canister corrosion). Currently salt, clay and granite are
31 considered as potential host rocks for a nuclear waste disposal in Germany. Microorganisms are
32 indigenous present in such subterranean environments and it was demonstrated that they can affect the
33 speciation and hence the mobility of An in different ways (e.g. Lloyd and Gadd 2011; Swanson et al.
34 2012; Lütke et al. 2013; Wouters et al. 2013; Moll et al. 2014).

35 The impact of microbes and their secreted substances on the plutonium mobility and migration was
36 highlighted in a recent review by Kersting (Kersting 2013). The need for a better mechanistic
37 understanding for Pu at the molecular level to understand for instance its transport behaviour was pointed
38 out. Plutonium as a redox sensitive element possesses a complicated chemistry because it can coexist in
39 several oxidation states, i.e., +3, +4, +5 and +6, in aqueous solution under environmental conditions.
40 Figure 1 depicts a generalized Eh – pH diagram that shows the dominant Pu species that exist for a range
41 of Eh and pH values calculated under anaerobic conditions. Hence the mobility of plutonium depends on
42 its speciation and is highly influenced by its oxidation state. The plutonium speciation can be affected by
43 environmental bacteria in terms of ligand complexation, internal accumulation or uptake, external
44 accumulation (e.g., biosorption), metal reduction and oxidation, and biomineralization through direct
45 (enzymatic) (e.g. Kimber et al. 2012; Ohnuki et al. 2009 and 2010; Reed et al. 2007; Boukhalfa et al.
46 2007; Icopini et al. 2009) and indirect redox transformations (e.g. Neu et al. 2005; Lukšienė et al. 2012).
47 Due to the diversity of microorganisms and the complexity of biogeochemical systems a wide range of
48 bacterially mediated processes occurred (Neu et al. 2010; Newsome et al. 2014). For instance, the
49 addition of citric acid and glucose to contaminated soil from the Nevada Test Site (NTS) stimulated
50 indigenous microbial activity and enhanced the dissolution of Pu under aerobic and anaerobic conditions
51 (Francis and Dodge 2015). The understanding of reactions between priority radionuclides such as Pu with
52 microbes and on mineral surfaces is essential for the safe management of radioactive wastes in order to
53 contribute to the remediation of radionuclide-contaminated land (Roh et al. 2015; Brookshaw et al. 2012).
54 The sorption of Pu may involve adsorption of oxidized species including a combination of reduction and
55 disproportionation reactions. Furthermore, Pu(V) and Pu(VI) can be reduced biotically to Pu(IV).

56 However, the role of complexing ligands in facilitating microbial reduction of Pu(VI) to Pu(III), and
57 enhancing Pu(III) solubility is not well understood at present. At near-neutral pH residual organics,
58 present in biologically active systems of *Shewanella alga* BrY, enzymatically reduce Pu(VI) to Pu(V)
59 (Reed et al. 2007). Several aerobic and anaerobic bacteria (e.g. *Bacillus* sp., *Pseudomonas* sp.,
60 *Citrobacter* sp., and *Clostridium* sp.) were isolated from for instance leachate samples collected from for
61 instance Pu contaminated soils (Francis 2007). Viable metabolically active microbes were detected at the
62 Los Alamos (LANL), transuranic (TRU) waste burial site containing ²³⁹Pu contaminated soil. A slight
63 increase in microbial activity (respiration) can alter the redox potential and reduce Pu(VI) to Pu(V). Since
64 the solubility of Pu(III) hydroxide is much greater a reduction of Pu(IV) oxyhydroxides to Pu(III)
65 hydroxide is expected to increase the solubility of Pu in the environment. A reductive dissolution of
66 Pu(IV) to Pu(III) by *Clostridium* sp. was observed (Francis et al. 2007 and 2008). Although Pu generally
67 exists as insoluble Pu(IV) in the environment, under appropriate conditions, anaerobic microbial activity
68 could affect the long-term stability and mobility of Pu by its reductive dissolution. The impact of the
69 Fe(III)-reducing bacteria *Geobacter sulfurreducens* and *Shewanella oneidensis* MR-1 on the speciation of
70 plutonium was investigated in (Renshaw et al. 2009). The results showed that in all cases, the presence of
71 bacterial cells enhanced removal of Pu from solution. It could be demonstrated that the sorbed and
72 precipitated Pu was mainly Pu(IV), but Pu(III) was also present. Hence, the microbial interactions with
73 plutonium are complex and driven by a combination of initial sorption to the cell surface, followed by
74 varying degrees of reduction, shown for Pu(VI) with *G. sulfurreducens* and for Pu(IV) with other bacteria
75 studied. In our previous study, we investigated the interaction of plutonium in mixed oxidation states
76 (Pu(VI) and Pu(IV)-polymers) with cells of the sulfate-reducing bacterial (SRB) strain *Desulfovibrio*
77 *äspöensis* DSM 10631^T, which frequently occurs in the deep granitic rock aquifers at the Äspö Hard Rock
78 Laboratory (Äspö HRL), Sweden (Moll et al. 2006). At high initial Pu concentrations between 620 to
79 1033 µM and a dry biomass concentration of 1 g/L, the experiments showed that the cells could
80 accumulate 18 ± 2 mg Pu / g_{dry weight} at pH 5. We used solvent extractions, UV-vis absorption
81 spectroscopy and X-ray absorption near edge structure (XANES) spectroscopy to determine the
82 speciation of Pu oxidation states. Extended X-ray absorption fine structure (EXAFS) spectroscopy was
83 used to study the coordination of the Pu bound by the bacteria. In the first step, the Pu(VI) and Pu(IV)-
84 polymers are bound to the biomass. Solvent extractions showed that 97 % of the initially present Pu(VI) is
85 reduced to Pu(V) due to the activity of the cells within the first 24 h of contact time. Most of the formed

86 Pu(V) dissolves from the cell envelope back to the aqueous solution due to the weak complexing
87 properties of this plutonium oxidation state.

88 The Opalinus Clay layer of the Mont Terri Underground Rock Laboratory (URL) is one potential
89 host rock tested for nuclear waste disposal in Switzerland (Thury and Bossart 1999). The here
90 investigated *Sporomusa* sp. MT-2.99 was recently isolated from Opalinus Clay core samples, collected
91 from a borehole of the Mont Terri URL, Switzerland (Bachvarova et al. 2009). However, so far very little
92 is known about the microbial activity in Mont Terri Opalinus Clay (Poulain et al. 2008) representing
93 unfavorable living conditions as the lack of water and nutrients and small pores. Recently, indigenous
94 bacteria from Mont Terri Opalinus Clay and its interactions with uranium, europium, and curium were
95 investigated (Lütke et al. 2013; Moll et al. 2014). These studies demonstrated the ability of the two
96 isolated strains *Sporomusa* sp. MT-2.99 and *Paenibacillus* sp. MT-2.2 to interact with An/Ln and hence to
97 change whose speciation and migration characteristics.

98 In this study, research was focused on the unknown interaction of *Sporomusa* sp. MT-2.99 with
99 plutonium. The accumulation of ^{242}Pu by the bacteria was investigated in dependence on the contact time,
100 the initial plutonium concentration, $[\text{}^{242}\text{Pu}]_{\text{initial}}$, within a pH range of 3 to 7 without and with adding Na-
101 pyruvate as electron donor under strict anaerobic conditions due to the physiological needs of the studied
102 bacterium. Solvent extractions and partly absorption spectroscopy were applied to explore the time
103 dependent ^{242}Pu oxidation state distribution a) in the blanks, b) the supernatants after separating from the
104 cells and c) of the Pu bound on the bacteria.

105

106 **Materials and Methods**

107

108 **Cultivation of bacteria**

109 *Sporomusa* sp. MT-2.99 was isolated from the Mont Terri Opalinus Clay core samples collected from
110 borehole BHT-1 from the Mont Terri URL, Switzerland (Bachvarova et al. 2009). For Pu interaction
111 studies *Sporomusa* sp. MT-2.99 was grown under anaerobic conditions (N_2 atmosphere) in liquid R2A
112 medium (DSMZ medium 830) at 30°C. The cells were grown to the late exponential growth phase and
113 harvested by centrifugation (8000xg). For plutonium interaction experiments under anaerobic conditions
114 the cells were washed three times and re-suspended in degassed analytical grade 0.9 % NaCl (Sigma-

115 Aldrich, Germany) solution containing 10^{-4} M Na-pyruvate (Sigma-Aldrich, Germany), respectively. The
116 biomass of the cell stock suspension was determined by measuring the OD_{600} , which was then converted
117 to the dry biomass according as described in Moll et al. 2014. The cell morphology and purity of the
118 strain of each used cell stock suspension was examined as described elsewhere (Moll et al. 2014).

119

120 Pu solution and quantification of Pu oxidation states by solvent extraction

121 The starting compound to obtain the ^{242}Pu stock solution was a green-brown powder of PuO_2 (AEA
122 technology QSA GmbH) with the following composition: 0.009 % of Pu-238, 0.008 % Pu-239, 0.020 %
123 Pu-240, 0.017 % Pu-241, 99.945 % Pu-242, and 0.001 % Pu-244. The problem is that this substance is
124 chemically highly inert and dissolves extremely slowly in acids (Keller 1971). We performed an oxidative
125 dissolution of $^{242}\text{PuO}_2$ in HNO_3 in the presence of AgNO_3 and $\text{K}_2\text{S}_2\text{O}_8$. Finally the $^{242}\text{Pu(VI)}$ stock
126 solution in 3 M HClO_4 was prepared by electrolysis. Because of the low absorption coefficients of
127 Pu(IV), Pu(V), and Pu(IV)-polymers (Keller 1971; Wilson et al. 2005; Ockenden and Welch 1956) and
128 the low concentration of Pu in the solutions, the quantification of the different Pu oxidation states was
129 performed by solvent extraction by a procedure adapted from (Nitsche et al. 1988 and Nitsche et al. 1994)
130 which was successfully applied in our previous study as described in (Moll et al. 2006). The extractions
131 were performed rapidly and in parallel. The pH of the extraction samples was 0 or 1. Hence, the
132 extraction procedure should not be affected by Pu hydrolysis. No hydrolysis dependence was reported in
133 the original references (Nitsche et al. 1988 and Nitsche et al. 1994). From the LSC-measurements, we
134 used the Pu-242 activity in each sample in order to calculate the fractions of the individual Pu oxidation
135 states. Therefore, all fractions are given in activity %.

136

137 Ultraviolet-visible-near infrared (UV-vis-NIR) absorption spectroscopy and liquid 138 scintillation counting

139 Besides solvent extraction in selected samples the plutonium oxidation state distribution was checked
140 by absorption spectroscopy in the ultraviolet-visible-near infrared (UV-vis-NIR) wavelength range. The
141 absorption spectroscopy measurements were performed using a CARY5G UV-vis-NIR spectrometer
142 (Varian Co.) at a temperature of 22 ± 1 °C. All plutonium concentrations were measured by liquid
143 scintillation counting (LSC) using a LS counter, Wallac system 1414 (Perkin Elmer). For this, defined

144 sample volumes (50 to 300 μL) were mixed with 5 mL of Ultima Gold scintillation cocktail (Sigma-
145 Aldrich, Germany). The solvent extraction experiments demonstrated that the acidic Pu stock solution still
146 contained, besides 73 % Pu(VI), 5 % Pu(III), and 19 % Pu(IV)-polymers due to the synthesis procedure.

147

148

149 pH and redox potential measurements

150 The pH was measured using an InLab Solids electrode (Mettler-Toledo, Giessen, Germany) calibrated
151 with standard buffers and a pH meter (Microprocessor pH Meter pH 537, WTW, Weinheim, Germany).
152 The pH was adjusted with a precision of 0.05 units. The pH adjustments were made with HClO_4 or NaOH
153 both from Merck, Germany. The redox potential in blanks and cell suspensions was measured using a
154 combination redox electrode (BlueLine 31 Rx from Schott, Germany) by applying the single point
155 calibration using a redox buffer. The electrode was calibrated by measuring the potential in the redox
156 buffer prior the Pu containing samples. The resulting error of the redox potentials was within 5 to 10 % of
157 the given values. The error was derived from repeated measurements including small systematic drifts of
158 the redox buffer.

159

160 Pu-bacteria interaction experiments

161 The Pu-bacteria interaction experiments were performed at [dry biomass] of $0.33 \pm 0.01 \text{ g}_{\text{dry weight}}/\text{L}$
162 and pH values of 3, 4, 6.1 and 7 under N_2 atmosphere at 25 °C in 0.1 M NaClO_4 solution. ^{242}Pu initial was
163 varied between 0.8 and 455 μM . Na-pyruvate (Sigma-Aldrich, Germany), as one potential electron donor
164 was added in two concentrations (0.1 and 10 mM) at pH 6.1. At pH 4 only one Na-pyruvate concentration
165 (10 mM) was added. Samples were taken after defined time steps. The separation of cells from the
166 supernatant solution was performed by centrifugation (6000xg). The ^{242}Pu present in blank (no cells
167 added), supernatant, and washed biomass suspension at pH 0 was analyzed using solvent extraction, and
168 LSC as described above.

169 The adsorption of Pu onto the reaction vessel as source of error was investigated as well. Therefore,
170 after the Pu interaction experiments the reaction tubes were rinsed 3 times with Milli-Q water and then
171 incubated for 2 days with 1 M HClO_4 to desorb Pu. Solutions were then analyzed with LSC regarding
172 [Pu]. The determined loss of Pu was accounted for the calculation of the amount of Pu bound per g dry

173 biomass.

174

175 Data analysis

176 The data evaluation was performed using the OriginPro 8.6G (OriginLab Corporation, USA) code.

177 The time-dependent Pu concentrations measured in the supernatants were successfully fitted with bi-

178 exponential decay functions. The time-dependent Pu oxidation state distributions were successfully fitted

179 by using mono-exponential decay or growth functions.

180

181 Results

182

183 Accumulation of Plutonium (^{242}Pu) by *Sporomusa* sp. as a function of pH

184 Our aim was to study the interaction process of Pu with *Sporomusa* sp. cells within a broad pH-range

185 from the acidic up to the near-neutral pH region (pH 3, 4, 6.1, and 7). The pH of Mont Terri Opalinus

186 Clay waters is expected to be in the neutral pH region (e.g. Joseph et al. 2013). A further reason for the

187 chosen pH-range was to keep the investigations with Pu comparable with our previous studies of U(VI)

188 interactions with the Mont Terri Opalinus Clay isolate *Paenibacillus* sp. (Lütke et al. 2013).

189 More Pu was removed by *Sporomusa* sp. MT-2.99 cells at pH 6.1 compared with the results measured

190 at pH 4.0 especially in the absence of Na-pyruvate (cf. Figure 2 a and b). The time-dependent behavior of

191 Pu in the supernatants was bi-exponential fitted ($y = y_0 + A_1 e^{-(x/t_1)} + A_2 e^{-(x/t_2)}$). The kinetic fits showed

192 that the overall process consists of at least two parts: a fast process having a time frame of ~ 0.5 h (e.g.,

193 biosorption) and a much slower process with a time frame of ~ 1000 h. At pH 4 and at initial Pu

194 concentrations of 190 and 460 μM (cf. Figure S1), it seems that *Sporomusa* has a slightly different

195 strategy to avoid the stress caused by Pu compared with pH 6.1. For example at $[\text{Pu}]_{\text{initial}} 190 \mu\text{M}$ after 2 h

196 of contact time a strong decrease of the Pu concentration in solution was measured. The cells could

197 release approximately 19 % of this bound Pu. It suggests that the cells could protect themselves for 24 h

198 from the Pu. At incubation times ≥ 24 h an exponential decrease of the Pu concentration in solution was

199 detected. This behavior was observed in all time-dependent experiments performed as a function of the

200 initial Pu concentration.

201 The biosorption of Pu on *Sporomusa* sp. MT-2.99 cells was evaluated using the Langmuir absorption

202 isotherm model (cf. Figure 2c). The application of the Langmuir-isotherm model in order to describe the
203 biosorption of heavy metals in biological systems (e.g. biosorption of heavy metals on algae) was reported
204 for instance in (Klimmek 2003). At pH 6.1 the maximal Pu loading on *Sporomusa* sp. cells was calculated
205 to be 230 mg Pu / g_{dry weight} compared to 160 mg Pu / g_{dry weight} at pH 4 (cf. Figure 2 c). The Langmuir
206 constant b describes the affinity of the adsorbed metal to the bacterial surface (Kümmel and Worch 1990;
207 Atkins 1998). The data showed that at pH 6.1 Pu has a 6 times higher affinity to the *Sporomusa* sp. MT-
208 2.99 surface compared to pH 4. Panak and Nitsche (2001) reported that aerobic soil bacteria *B. sphaericus*
209 and *P. stutzeri* accumulated between 30 and 75 mg Pu / g_{dry weight} under comparable conditions at pH 5.
210 This shows that *Sporomusa* sp. accumulated relatively high amounts of Pu. Additionally, *Sporomusa* sp.
211 cells displayed a strong pH-dependent affinity for Pu (cf. Figure 2). At pH 3, only 13 % of the initial Pu
212 was accumulated whereas at pH 7, 90 % were associated with the biomass (cf. Figure S2).

213

214 Accumulation of Plutonium (²⁴²Pu) by *Sporomusa* sp. cells depending on addition of 215 Na-pyruvate

216 Na-pyruvate was used as electron donor because characterization tests showed that this carbon
217 source was best digested by the bacteria. The electron donor was used in the concentration range between
218 11 and 1100 mg/l. The total organic carbon (TOC) content of Mont Terri Opalinus Clay waters vary
219 between 19 and 58 mg/l (Thury and Bossart 1999). The composition of the TOC is not known in detail at
220 the moment.

221 At pH 4 the kinetic fits showed that the overall process consists of at least two parts: a fast process
222 having a time frame of ~ 0.1 h (e.g., biosorption) and a much slower process with a time frame of ~ 120 h
223 (cf. Figure S3a). We observed faster processes compared with the results when no Na-pyruvate was
224 added. One reason for this observation could be the different Pu speciation and Pu redox chemistry in the
225 presence of Na-pyruvate. At pH 6.1 the time-dependent decrease of Pu could be best fitted applying a
226 mono-exponential decay law. This indicates one dominating step having a short time frame of 8.3 h (cf.
227 Figure S3b).

228 A comparison of the cell bound Pu in dependence on pH and Na-pyruvate concentration was done
229 with [Pu]_{initial} of 57.8 µM. The accumulated amount of Pu was calculated based on the fit of the time-
230 dependent Pu concentrations in the corresponding solution. At pH 4 in the absence of Na-pyruvate 24.4 ±
231 1.2 mg Pu / g_{dry weight} was accumulated compared with 20.5 ± 0.7 mg Pu / g_{dry weight} in the presence of 10

232 mM Na-pyruvate. At pH 6.1 the cells accumulated 45 ± 5 mg Pu / g_{dry weight} in pure 0.1 M NaClO₄, 42 ± 6
233 mg Pu / g_{dry weight} in the presence of 0.1 mM Na-pyruvate, and only 26 ± 1 mg Pu / g_{dry weight} when 10 mM
234 Na-pyruvate was present. The observed effect was highest at pH 6.1. Here, approximately half of the Pu
235 amount was accumulated in the presence of 10 mM Na-pyruvate compared with the amount detected in
236 the absence of Na-pyruvate. The observed differences in the bioassociation behavior of Pu might be
237 related to the corresponding Pu speciation and redox chemistry in the presence and absence of Na-
238 pyruvate. For example at pH 6.1 with 10 mM Na-pyruvate an increased amounts of Pu(III) (see next
239 sections) were formed. This Pu(III) remained more mobile and hence was not associated on the biomass.
240 Processes forming mobile Pu(III) in the presence of microbes were discussed in (e.g. Francis et al. 2007
241 and 2008, Boukhalfa et al. 2007). Up to present, we could not find any information of stability constants
242 describing soluble Pu-pyruvate species. The lower tendency of bioassociation can be also explained by
243 the formation of soluble Pu(III) (cf. Figure 3 C). Similar effects were observed by Boukhalfa et al. in their
244 investigations with *G. metallireducens* GS-15 and *S. oneidensis* MR-1 (Boukhalfa et al. 2007).

245

246 Reversibility of Pu bioassociation

247 To estimate the reversibility of the Pu bioassociation process, the Pu loaded biomasses were treated
248 with 1 M HClO₄ in order to determine the amount of extractable Pu. In the absence of Na-pyruvate only
249 40 % of the plutonium was released at pH 6.1. In general, similar results were obtained at pH 4. These
250 findings indicated that the interaction process is only partly reversible. Beside the formation of surface
251 complexes with functional groups of the cell surface, and bio-reduction reactions other process can take
252 place (e.g. emplacement in cell membrane structures). Also for Cm(III) and Eu(III) a certain amount (30
253 to 40 %) was identified to be irreversibly bound to the cells (Moll et al. 2014). At pH 4 in two samples the
254 acidified biomasses were treated with 0.01 M EDTA at pH 5. In average 31 ± 3 % of the strongly bound
255 Pu could be released. Hence, 69 % of the irreversibly bound Pu remained on the biomass indicating a
256 strong interaction with the cells. In contrast to the electron donor free experiments, we could measure that
257 more than 80 % of the plutonium was released from the cells in the presence of 10 mM Na-pyruvate at pH
258 6.1. This might indicate a dominant complexation/fixation of plutonium on functional groups located at
259 the cell surface. Desorption experiments were performed as a function of the pyruvate concentration. The
260 average amounts of extractable Pu from the cells at [Pu]_{initial} 58 μM were: 41 ± 7 % no donor, 55 ± 11 %
261 0.1 mM pyruvate, and 93 ± 3 % 10 mM pyruvate. This showed that increased concentrations of pyruvate

262 increase also the contribution of a reversible surface complexation of Pu on the bacterial cell surface.

263

264 Redox potential measurements

265 Under steady state conditions, at $[\text{Pu}]_{\text{initial}}$ of 180 μM in the biomass suspensions redox potentials of
266 800 ± 40 , 700 ± 35 , 425 ± 21 , and 535 ± 27 mV were measured at pH 3, 4, 6.1, and 7, respectively (cf.
267 Figure 1). In the blanks were always measured higher redox potentials of 1020 ± 76 , 1040 ± 78 , 790 ± 75 ,
268 and 870 ± 65 mV, respectively at the corresponding pH values. Hence, the redox potential measurements
269 indicated that the cells generated reducing conditions. The cell induced effect on the redox potential was
270 highest at pH 6.1. Hence, the ability of the cells to decrease the redox potential depends on the pH.
271 Concerning the time dependence at pH 6.1, in the blank sample at $t \geq 312$ h a redox potential of
272 790 ± 73 mV was measured. In the cell suspensions immediately a constant value of 424 ± 21 mV was
273 reached. The ability of the cells to reduce the redox potential in Pu containing cell suspensions depends
274 also on the Pu concentration present. Because at pH 6.1 under steady state conditions and at $[\text{Pu}]_{\text{initial}}$ 62
275 μM and 454 μM the redox potential was measured to be 331 mV and 633 mV, respectively. The cell
276 induced effect on the redox potential is smaller in the presence of 10 mM Na-pyruvate. Based on the
277 redox potential measurements and besides abiotic reduction process of for instance Pu(VI) a cell induced
278 effect on the time-dependent Pu oxidation state distribution is likely to occur and will be discussed in the
279 following paragraph.

280

281 Time-dependent Pu oxidation state distributions – no electron donor

282 *The blank.* In the beginning the dominating Pu species are Pu(VI), 58 ± 7 %, Pu(IV)-polymers,
283 19 ± 1 % and Pu(III), 13 ± 6 % (see supplementary material Figure S4 a and b). The time-dependent
284 behavior of Pu(VI) and Pu(V) was mono-exponential fitted ($y = y_0 + A_1 e^{-(x/t)}$). The decrease of Pu(VI) at
285 pH 6.1 is 3.2 times faster than at pH 4. The increase of Pu(V) at pH 6.1 is 3.3 times faster than at pH 4. At
286 pH 6.1 and under steady state conditions the Pu(VI) amount decreased to 4 ± 1 %, the Pu(V) amount
287 increased to 76 ± 4 % and the Pu(IV)-polymer amount was 13 ± 4 %. The dominance of Pu(V) was also
288 predicted in the Eh – pH calculations shown in Figure 1. Whereas at pH 4 under steady state conditions,
289 higher amounts of Pu(VI) of 23.5 ± 2 %, lower amounts of Pu(V) of 57 ± 2 % were measured. The Eh –
290 pH calculations predicted a dominance of Pu(VI) (cf. Figure 1). Here, the Pu(IV)-polymer amount
291 remains constant at 19.6 ± 0.8 % within the investigated time range. Concluding that a more acidic pH

292 stabilizes Pu(VI). This observation is in agreement with the Eh-pH calculations shown in Figure 1.

293 *The supernatant.* A significant change of the Pu oxidation state distributions was observed in the
294 supernatants (cf. Figure 3 a and supplementary material Figure S4 c) compared with the blanks. At both
295 pH values a fast decrease of Pu(VI) combined with a fast increase of Pu(V) was observed. At pH 6.1 the
296 formation of Pu(V) in the supernatant is 48 times faster than in blank samples. Whereas the decrease of
297 Pu(VI) in the supernatant is 28 times faster than in the blanks. The increase in the Pu(V) concentration is
298 faster than expected. Because one should assume an equilibrium between the formation of Pu(V) and the
299 decrease of Pu(VI) as observed in the blanks. One explanation could be the influence of the cells on the
300 observed processes. At pH 6.1, the equilibrium concentration of Pu(V) in the supernatants is with ca.
301 90 % higher than in the blanks where 76 % was found. At pH 4 the formation of Pu(V) in the supernatant
302 is 144 times faster than in blank samples. The decrease of Pu(VI) in the supernatant is 626 times faster
303 than in the blanks. The decrease of Pu(VI) was much faster compared with the increase of Pu(V). Again,
304 this discrepancy from equilibrium might be explained by the influence of the cells. The observed cell
305 mediated reduction process of Pu(VI) to Pu(V) is not yet fully understood. After the interaction the
306 majority of the Pu(V) was detected in solution (cf. Table 1). We assume that this happens due to the
307 comparable weak complexing properties of the PuO_2^+ ion which is related with a release from the cell
308 envelope. Similar observations were made in the past (Panak and Nitsche 2001; Moll et al. 2006). The
309 formed Pu(V) is relatively stable after removing the cells from solution. The dominance of Pu(V) in the
310 supernatants/cell suspensions is also in agreement with the Eh-pH calculations shown in Figure 1 (for pH
311 3, 4, and 7). For the cell suspension at pH 6.1 predominantly Pu(IV) was predicted (cf. Figure 1). This
312 could not be confirmed experimentally due to the dominance of Pu(V). At pH 6.1 the equilibrium
313 concentration of the Pu(IV)-polymers was 6 % compared with 12.5 % found in the blanks. This suggests a
314 pronounced biosorption of Pu(VI)-polymers on the biomass.

315 *UV-vis-NIR spectroscopy:* The time-dependent decrease of Pu(VI) (cf. Figure 4 a) and the increase
316 of Pu(V) (cf. Figure 4 b) could be confirmed by UV-vis-NIR spectroscopy. The absorption band at 830
317 nm is associated with the PuO_2^{2+} ion (e.g. Cho et al. 2010). Red shifted absorption bands appear at around
318 848 and 858 nm, which suggested the formation of Pu(VI) hydrolysis species. The absorption band
319 position of 848 nm suggested the occurrence of polynuclear hydrolysis species like $(\text{PuO}_2)_2(\text{OH})_2^{2+}$ (e.g.
320 Reilly and Neu 2006). Those species are formed in the millimolar Pu(VI) concentration range. Whereas at
321 lower Pu(VI) concentrations below 10^{-4} M the monomeric species are dominant. The absorption band

322 detected at 848 nm is most likely the sum signal from PuO_2OH^+ and $(\text{PuO}_2)_2(\text{OH})_2^{2+}$. The shoulder
323 detected at 858 nm might indicate the influence of $\text{PuO}_2(\text{OH})_2$ (aq) which is characterized by an
324 absorption band at 850.3 nm (e.g. Cho et al. 2010). At pH 6.1 and based on the results coming from the
325 absorption spectra the cells are interacting mainly with Pu(VI)-hydrolysis species. The signal of PuO_2^{2+}
326 decreased much faster than the sum signal of the Pu(VI)-hydroxo species (cf. Figure 4 a left). This could
327 mean that PuO_2^{2+} showed a higher affinity to sorb on the bacterial surface. At incubation times > 49 hours
328 no safe prediction can be made regarding the Pu(VI) amount in the supernatant. The decrease of the
329 Pu(VI) signal is much faster than in the blank samples (cf. Figure 4 a right). As a function of the
330 incubation time we detected an increase of the typical absorption band of Pu(V) at 569 nm (cf. Figure 4
331 b).

332 *Biomass.* The summary of all extraction data observed in the electron-donor free experiments with
333 *Sporomusa* sp. showed scattered concentration data of the individual plutonium oxidation states (cf.
334 Figure S5a). No differences of the time-dependent Pu oxidation state distributions were detected as a
335 function of $[\text{Pu}]_{\text{initial}}$. The exponential decay functions shown in Figure S5a were only used to estimate the
336 average amount of the individual Pu oxidation states. No defined time dependencies of the Pu oxidation
337 states could be seen from the measurements (cf. Figure S5a). Therefore, the steady state concentrations of
338 the major Pu oxidation states identified on the biomass are depicted in Figure 3 b. At pH 6.1 the major Pu
339 oxidation state was Pu(IV)-polymers with an average amount of 42 ± 4 %. Also at pH 4 the tetravalent Pu
340 dominates (37 % Pu(IV) and 25 % Pu(IV)-polymers). The Pu(III) average amount of 27 % at pH 6.1 is
341 clearly higher than found in the blanks and supernatants. At both pH values the fraction of Pu which was
342 not accessible by the extraction technique amounted to 30 %. This plutonium could be masked for
343 instance by an uptake in biomass. And can be also correlated with the amount of irreversibly bond Pu
344 (*Sporomusa* sp.: 40 - 60 %).

345

346 Time-dependent Pu oxidation state distributions – with electron donor

347 *The blank.* Compared to the pyruvate-free system (cf. supplementary material Figure S6 a and b) a
348 more complex Pu redox-chemistry was observed. The observed changes in the individual Pu oxidation
349 states are triggered by both natural occurring reduction/oxidation reactions (as depicted in Figure S4 a and
350 b) and reduction processes promoted by Na-pyruvate (cf. supplementary material Figure S6 a and b). At
351 the beginning at pH 6.1, the major oxidation states (complexed with pyruvate) interacting with the

352 biomass are Pu(V) with 31 %, Pu(IV) with 22 %, and Pu(IV)-polymers with 23 %. At the beginning at pH
353 4, the major oxidation states (complexed with pyruvate) interacting with the biomass are Pu(IV) with
354 39 %, Pu(V) with 20 %, and Pu(IV)-polymers with 24 %. At pH 6.1 within the first 1.2 h the amount of
355 Pu(VI) decreased from 61 % to about 4 %. At pH 4 after 2 h almost no Pu(VI) could be detected. At both
356 pH values simultaneously Pu(V) and Pu(IV) increased to about 31 % (22 % at pH 4) and 22 % (45 % at
357 pH 4), respectively. At pH of 6.1, we observed also an increase of Pu(IV)-polymers from 19 % in the
358 beginning to about 34 % at the end of the experiment. This could be explained by a transfer of the formed
359 Pu(IV) into Pu(IV)-polymers at this pH. At pH 4 the Pu(IV)-polymer fraction remained constant at $27 \pm$
360 3 %. Pu(V) was abiotically reduced to Pu(IV) due to the presence of pyruvate. Later on ($t \geq 144$ h) an
361 increase of Pu(III) in combination with an decrease of Pu(IV) at pH 6.1 was observed (cf. Figure S6 b).
362 This might indicate a further reduction of Pu(IV) forming Pu(III). Hence, to model the Pu(IV) behavior at
363 pH 6 the data were split into two time ranges. First, there was an exponential growth of Pu(IV) followed
364 by an exponential decrease. In contrast at pH 4, there was an exponential growth of the Pu(IV) fraction
365 with a steady state concentration of 70 % (major difference between both pH values). At pH 6.1 an
366 exponential growth of Pu(III) with an equilibrium concentration of 55 % was calculated. Whereas at pH 4
367 for a very low Pu(III) equilibrium concentration of ca. 0.1 % was found.

368 *The supernatant.* At pH 6.1 a similar behavior of dominating Pu oxidation states could be observed
369 as found in the blanks (cf. Figure 3 c and S6 d). However, due to cell induced effects the formation of
370 Pu(III) as the major oxidation state is 68 times faster than in blank samples. The decrease of Pu(IV) in the
371 supernatant is 9 times faster than in the blanks. The decrease of Pu(V) is 35 times faster than in the blank
372 samples. Under steady state conditions similar concentrations of Pu(III) (~50 %), Pu(IV) (~15 %), and
373 Pu(V) (~1 %) were measured in blanks and the *Sporomusa* sp. supernatants. In contrast to pH 6.1 at pH 4
374 in the *Sporomusa* sp. system a clear enrichment of Pu(IV) was observed (cf. Figure S6 c). At pH 4 the
375 main difference compared to the blanks due to cell mediated processes was a faster increase of Pu(IV) (33
376 times), and slightly lower concentrations of Pu(IV)-polymers (23.2 %).

377 *The biomass.* At pH 6.1 there was a clear enrichment of Pu(III) in the biomass in the presence of 10
378 mM Na-pyruvate (Figure 3 d and Figure S5 b), whereas Pu(IV)-polymers associated on biomass
379 dominated in in the sample without additional electron donor (Figure 3 b). A steady state concentration of
380 70 ± 4 % for Pu(III) was observed. This amount is three times higher than in the electron donor free
381 system. In the presence of Na-pyruvate, the Pu(IV)-polymer concentration in the biomass yielded lower

382 steady state concentrations than in the electron donor free experiments. Therefore, we assume a transfer of
383 Pu(IV)-polymers into Pu(III) promoted by pyruvate and by reducing electrochemical zones provided by
384 the bacterial cell membrane (e.g. Neu et al. 2005). From the pyruvate concentration-dependent
385 experiments one can conclude that 0.011 g/L pyruvate has a similar influence on the Pu redox chemistry
386 as 0.33 g/L *Sporomusa* sp. MT-2.99 cells. The decrease of the Pu(IV)-polymer amount is approximately 4
387 times faster at pH 6.1 compared to pH 4. The equilibrium amount is with 23.5 % equal for both pH
388 values. The main difference (as also observed in the blank and the supernatants) is an enrichment of
389 Pu(IV) on the biomass at pH 4 (cf. Figure 3 d and S6 e), whereas Pu(III) was enriched at pH 6.1.

390

391 **Discussions**

392

393 *0.1 M NaClO₄ no donor.* A very fast decrease of Pu(VI) in solution in the presence of cells was
394 observed (cf. Figure S4 C and D; Figure 3 a). This process is connected with a fast increase of Pu(V).
395 However, this Pu(V) was not observed on the cells. There must be a fast reduction (cell promoted because
396 it was faster than in the blanks) forming Pu(V) in the vicinity of the cells or at the cell surface after a fast
397 bioassociation of Pu(VI) (cf. Figure 5). Under steady state conditions the equilibrium concentration of
398 Pu(VI) was 4.1 μ M (0.04 μ M at pH 6.1) in the supernatants not interacting with the cells. A clear
399 enrichment of Pu(IV)-polymers on the biomass could be seen (cf. Table 1) especially at pH 6.1. Here, the
400 Pu(IV)-polymer concentration is higher on the biomass in comparison to blanks and supernatants. The
401 cells could induce a transformation process forming Pu(IV)-polymers from the sorbed Pu(IV). In a first
402 very fast step there was most likely an association of Pu(VI) and Pu(IV)-polymers at the cell envelope
403 followed by a reduction forming Pu(V). This process is ca. 48 times faster than in blank samples. Ohnuki
404 et al. reported also the reduction of Pu(VI) to Pu(V) in their experiments with *B. subtilis* with and without
405 kaolinite clay (Ohnuki et al. 2009). The observed second step the reduction of Pu(V) to Pu(IV) was not
406 observed in our experiments. Pu(V) identified in the supernatants can disproportionate in aqueous
407 solution forming Pu(IV) and Pu(VI) (e.g. Nitsche et al. 1988). Pu(VI) was found in the supernatants.
408 Whereas Pu(IV) was associated on the biomass. Part of this Pu(IV) could be further reduced to Pu(III). At
409 pH 6.1 we observed higher amounts of Pu(III) on the biomass compared with pH 4. Simultaneously lower
410 values of Pu(IV) were detected. Hence, there was a stronger tendency of a transformation of the
411 bioassociated Pu(IV) forming Pu(III). Here dead biomass might act as an electron donor. However, the

412 mechanism of this Pu(IV) reduction is not clear at the moment.

413 *10 mM Na-pyruvate pH 4.* The time-dependent Pu oxidation state distribution is driven by the
414 reducing properties of Na-pyruvate. Under steady state conditions (cf. Table 2) the concentration of
415 Pu(IV) in blanks was 40 μM . Approximately half of it, ca. 20 μM , was found in the supernatant and on
416 the biomass each. The formation of Pu(IV) in the supernatant was 68 times faster than in blanks. At the
417 beginning there was a biosorption of Pu(IV)-polymers on the biomass. This Pu(IV)-polymer fraction
418 decreased with time and was accompanied by an increase of Pu(IV). This Pu(IV) concentration can be a
419 result of the biosorption of Pu(IV) from the supernatant and/or of a biotransformation of Pu(IV)-polymers
420 into Pu(IV) in the biomass (cf. Figure 5). It is difficult to postulate a direct bioreduction of Pu(VI)
421 forming Pu(IV) by *Sporomusa* sp. cells. Interestingly, no further reduction of Pu(IV) to Pu(III) was
422 observed.

423 *10 mM Na-pyruvate pH 6.1.* At incubation times within 0 and 200 h in the blanks mainly Pu(IV) and
424 Pu(IV)-polymers were detected (cf. Figure S6 b). However, on the biomass the major Pu oxidation states
425 were always Pu(III) in addition to Pu(IV)-polymers. The formation of Pu(III) is 68 times faster in the
426 supernatants and 2 times faster on the cells compared with the dependencies in the blanks. First a
427 biosorption of Pu(IV) (and Pu(IV)-polymers) could be the initial step followed by a bioreduction forming
428 Pu(III). In addition a biotransformation of Pu(IV)-polymers into Pu(III) seems possible. The majority of
429 Pu(III) was found on the biomass (cf. Figure 5). One explanation would be a cell catalyzed bioreduction
430 process of Pu(IV) and Pu(IV)-polymers in the presence of 10 mM Na-pyruvate at pH 6.1. The potential of
431 microbes to reduce Pu(IV) to Pu(III) in the presence of electron donors was reported in (e.g. Boukhalfe et
432 al. 2007; Renshaw et al. 2009).

433

434 **Conclusions**

435

436 In this study, the interaction of Pu with the bacterium, *Sporomusa* sp. MT-2.99, isolated from Mont
437 Terri Opalinus Clay, was investigated in 0.1 M NaClO₄ as a function of the initial Pu concentration, the
438 pH, and with and without the addition of Na-pyruvate as an electron donor. In the electron donor
439 containing system faster kinetics were found. The isolate displayed a strong pH-dependent affinity for Pu.
440 Using the Langmuir model the maximal Pu loading at pH 6.1 on *Sporomusa* sp., $230 \pm 14 \text{ mg Pu} / \text{g}_{\text{dry}}$
441 _{weight}, was calculated. The maximal loadings are high compared to literature values (e.g. Panak and

442 Nitsche 2001; Moll et al. 2006). Hence, *Sporomusa* sp. cells were efficient in removing Pu from the
443 surrounding solution. In the presence *Sporomusa* sp. cells a change in the Pu oxidation state distributions
444 was discovered in comparison to the abiotic controls (cf. Figure 5). In the absence of added organics there
445 was a fast increase of Pu(V) in the cell suspensions. On the biomass an enrichment of Pu(IV)-polymers
446 independent of $[Pu]_{\text{initial}}$ and pH was observed. The dominance of Pu(V) in the cell suspensions could be
447 explained by the decrease of E_h , a possible release of complexing agents by the cells and by reducing
448 properties of the cells itself. For example a release of such agents was concluded for suspensions of the
449 Mont Terri Opalinus Clay isolate *Paenibacillus* sp. in the presence of U(VI) (Lütke et al. 2013). The role
450 of residual organics present in biologically active systems to reduce Pu(VI) species to Pu(V) species at
451 near-neutral pH was pointed out in Reed et al. 2007. The predominance of Pu(V) might indicate
452 biologically active systems at least in the starting phase of our experiments. In the presence of 10 mM Na-
453 pyruvate the Pu oxidation state distribution was pH-dependent. Under steady state conditions the redox
454 potential was measured to be ca. 480 mV in abiotic controls and cell suspensions at pH 4. Using Figure 1
455 as an approximate Pu(IV) should be the dominant oxidation state. Approximately 50 % remains in
456 solution of the cell suspensions and 50 % was associated with the cells. The influence of the cells is
457 pronounced in a faster enrichment of Pu(IV). At pH 6.1 again under steady state conditions the redox
458 potential in abiotic controls and cell suspensions was measured to be 190 mV. Using Figure 1 as an
459 approximate Pu(III) should be the dominant oxidation state. In agreement with the observations: 76 % of
460 Pu(III) was found on the biomass and 24 % in the supernatant. Therefore, the cells induced a faster
461 formation of Pu(III) compared to the abiotic controls.

462 To conclude, a moderate to strong impact of *Sporomusa* sp. cells on the Pu speciation was observed
463 (cf. Figure 5). The presented results contribute to a better mechanistic understanding of Pu
464 biogeochemistry in the presence of host rock indigenous bacterial cells.

465

466 **Acknowledgements**

467 The authors thank the BMWi for financial support (contract no.: 02E10618 and 02E10971), Velina
468 Bachvarova and Sonja Selenska-Pobell for isolation of the bacterial strain, Monika Dudek for strain
469 cultivation and the BGR for providing the clay samples. Thanks to Laura Lütke for valuable help in strain
470 characterization and many fruitful discussions as well as Susanne Sachs and Katja Schmeide for help in
471 preparing the Pu-242 stock solution.

472

473 **References**

474 Atkins PW (1998) Physical Chemistry. Oxford University Press, Oxford, UK.

475 Bachvarova V, Geissler A, Selenska-Pobell S (2009) Bacterial isolates cultured under anaerobic
476 conditions from an opalinus clay sample from the Mont Terri Rock laboratory. FZD-530 FZD-IRC
477 Annual Report, 18.

478 Bethke CM (2008) "Geochemical and Biogeochemical Reaction Modeling" 2nd Ed., Cambridge
479 University Press, 543 pp.

480 Boukhalfa H, Icopini GA, Reilly SD, Neu MP (2007) Plutonium(IV) reduction by the metal-reducing
481 bacteria *Geobacter metallireducens* GS-15 and *Shewanella oneidensis* MR-1. Appl Environ Microbiol
482 73:5897–5903.

483 Brookshaw DR, Patrick RAD, Lloyd JR, Vaughan DJ (2012) Microbial effects on mineral-radionuclide
484 interactions and radionuclide solid-phase capture processes. Mineral Mag 76:777–806.

485 Cho H-R, Jung EC, Park KK, Kim WH, Song K, Yun J-I (2010) Spectroscopic study on the mononuclear
486 hydrolysis species of Pu(VI) under oxidation conditions. Radiochim Acta 98:765–770.

487 Francis AJ (2007) Microbial mobilization and immobilization of plutonium. J Alloys Compd 444-
488 445:500-505.

489 Francis AJ, Dodge CJ, Gillow, JB (2008) Reductive dissolution of Pu(IV) by *Clostridium* sp. under
490 anaerobic conditions. Environ Sci Technol 42:2355-2360.

491 Francis AJ, Dodge CJ (2015) Microbial mobilization of plutonium and other actinides from contaminated
492 soil. J Environ Radioact 150:277-285.

493 Guillaumont R, Fanghänel T, Fuger J, Grenthe I, Neck V, Palmer DA, Rand MH (2003) Chemical
494 Thermodynamics Series Volume 5: Update on the Chemical Thermodynamics of Uranium,
495 Neptunium, Plutonium, Americium and Technetium, Elsevier, Amsterdam, 960 pp.

496 Icopini GA, Lack JG, Hersman LE, Neu MP, Boukhalfa H (2009) Plutonium(V/VI) reduction by the
497 metal-reducing bacteria *Geobacter metallireducens* GS-15 and *Shewanella oneidensis* MR-1. Appl
498 Environ Microbiol 75:3641–3647.

499 Joseph C, Van Loon LR, Jakob A, Steudtner R, Schmeide K, Sachs S, Bernhard (2013) Diffusion of
500 U(VI) in Opalinus Clay: Influence of temperature and humic acid. Geochim Cosmochim Acta 75:352–
501 367.

502 Keller C (1971) The Chemistry of the Transuranium Elements, Volume 3, Verlag Chemie GmbH,
503 Weinheim, Germany.

504 Kersting AB (2013) Plutonium transport in the environment. *Inorg Chem* 52:3533-3546.

505 Klimmek S (2003) Charakterisierung der Biosorption von Schwermetallen an Algen. PhD thesis,
506 Technische Universität Berlin, Berlin, Germany.

507 Kimber RL, Boothman C, Purdie P, Livens FR, Lloyd JR (2012) Biogeochemical behavior of plutonium
508 during anoxic biostimulation of contaminated sediments. *Mineral Mag* 76:567-578.

509 Kümmel R, Worch E (1990) Adsorption aus wässrigen Lösungen. Dt. Verl. für Grundstoffindustrie:
510 Leipzig, Germany.

511 Lemire RJ, Fuger J, Nitsche H, Potter P, Rand MH, Rydberg J, Spahiu K, Sullivan JC, Ullman W,
512 Vitorge P, Wanner H (2001) Chemical Thermodynamics Series Volume 4: Chemical
513 Thermodynamics of Neptunium and Plutonium, Elsevier, Amsterdam, 870 pp.

514 Lloyd JR, Gadd GM (2011) The Geomicrobiology of Radionuclides. *Geomicrobiol J* 28:383–386.

515 Lukšienė B, Druteikienė R, Pečiulytė D, Baltrūnas D, Remeikis V, Paškevičius A (2012) Effect of
516 microorganisms on the plutonium oxidation states. *Appl Radiat Isot* 70:442-449.

517 Lütke L, Moll H, Bachvarova V, Selenska-Pobell S, Bernhard G (2013) The U(VI) speciation influenced
518 by a novel *Paenibacillus* isolate from Mont Terri Opalinus clay. *Dalton Trans* 42:6979-6988.

519 Moll H, Merroun ML, Hennig Ch, Rossberg A, Selenska-Pobell S, Bernhard G (2006) The interaction of
520 *Desulfovibrio äspöensis* DSM 10631^T with plutonium. *Radiochim Acta* 94:815-824.

521 Moll H, Lütke L, Bachvarova V, Cherkouk A, Selenska-Pobell S, Bernhard G (2014) Interactions of the
522 Mont Terri Opalinus Clay Isolate *Sporomusa* sp. MT-2.99 with Curium(III) and Europium(III).
523 *Geomicrobiol J* 31:682-696.

524 Neu MP, Icopini GA, Boukhalfa H (2005) Plutonium speciation affected by environmental bacteria.
525 *Radiochim Acta* 93:705–714.

526 Neu MP, Boukhalfa H, Merroun ML (2010) Biomineralization and biotransformations of actinide
527 materials. *MRS Bulletin* 35:849–857.

528 Nitsche H, Lee SC, Gatti RC (1988) Determination of plutonium oxidation states at trace levels pertinent
529 to nuclear waste disposal. *J Radioanal Nucl Chem* 124:171–185.

530 Nitsche H, Roberts K, Xi R, Prussin T, Becraft K, Mahamid IA, Silber HB, Carpenter SA, Gatti RC
531 (1994) Long term plutonium solubility and speciation studies in a synthetic brine. *Radiochim Acta*

532 66/67:3–8.

533 Newsome L, Morris K, Lloyd JR (2014) The biogeochemistry and bioremediation of uranium and other
534 priority radionuclides. *Chem Geol* 363:164-184.

535 Ockenden DW, Welch GA (1956) The Preparation and Properties of Some Plutonium Compounds. Part
536 V.* Colloidal Quadrivalent Plutonium. *J Chem Soc* :3358–3363.

537 Ohnuki T, Yoshida T, Ozaki T, Kozai N, Sakamoto F, Nankawa T, Suzuki Y, Francis AJ (2009)
538 Modeling of the interaction of Pu(VI) with the mixture of microorganism and clay. *J Nucl Sci Technol*
539 46:55–59.

540 Ohnuki T, Kozai N, Sakamoto F, Ozaki T, Nankawa T, Suzuki Y, Francis AJ (2010) Association of
541 actinides with microorganisms and clay: Implications for radionuclide migration from waste-
542 repository sites. *Geomicrobiol J* 27:225–230.

543 Panak PJ, Nitsche H (2001) Interaction of aerobic soil bacteria with plutonium(VI). *Radiochim Acta*
544 89:499–504.

545 Poulain S, Sergeant C, Simonoff M, Le Marrec C, Altmann S (2008) Microbial investigations in opalinus
546 clay, an argillaceous formation under evaluation as a potential host rock for a radioactive waste
547 repository. *Geomicrobiol J* 25:240-249.

548 Reed DT, Pepper SE, Richmann MK, Smith G, Deo R, Rittmann BE (2007) Subsurface bio-mediated
549 reduction of higher-valent uranium and plutonium. *J Alloys Compd* 444-445:376–382.

550 Reilly SD, Neu MP (2006) Pu(VI) Hydrolysis: Further Evidence for a Dimeric Plutonyl Hydroxide and
551 Contrasts with U(VI) Chemistry. *Inorg Chem* 45:1839–1846.

552 Renshaw JC, Law N, Geissler A, Livens FR, Lloyd JR (2009) Impact of the Fe(III)-reducing bacteria
553 *Geobacter sulfurreducens* and *Shewanella oneidensis* on the speciation of plutonium.
554 *Biogeochemistry* 94:191–196.

555 Roh C, Kang C, Lloyd JR (2015) Microbial bioremediation processes for radioactive waste. *Korean J*
556 *Chem Eng* 32:1720-1726 and references therein.

557 Swanson JS, Reed DT, Ams DA, Norden D, Simmons KA (2012) Status report on the microbial
558 characterization of halite and groundwater samples from the WIPP, Los Alamos National Laboratory,
559 p. 1.

560 Thury M, Bossart P (1999) The Mont Terri Rock Laboratory, a new international research project in a
561 Mesozoic shale formation, in Switzerland. *Eng Geol* 52:347-359.

562 Wilson RE, Hu Y-J, Nitsche H (2005) Detection and quantification of Pu(III, IV, V, and VI) using a 1.0-
563 meter liquid core wave guide. *Radiochim Acta* 93:203-206.

564 Wouters K, Moors H, Boven P, Leys N (2013) Evidence and characteristics of a diverse and
565 metabolically active microbial community in deep subsurface clay borehole water. *FEMS Microb*
566 *Ecol* 86:458–473.

567

568

569 **Tables**

570 **Table 1** Quantification of the different Pu oxidation states in the *Sporomusa* sp. system determined by
 571 solvent extractions in combination with LSC in the 0.1 M NaClO₄ experiments under steady state
 572 conditions ([Pu]_{initial} 59 ± 4 μM).

573

	pH 4			pH 6		
	Blank	Supernatant	Biomass	Blank	Supernatant	Biomass
Pu(IV) μM	-	-	10.7	0.4	-	5.4
Pu(VI) μM	22.5	4.1	-	2.5	0.04	-
Pu(III) μM	-	-	5.3	3.7	-	16.7
Pu(V) μM	17.3	14.1	-	47.1	1.76	-
Pu(IV)-Polymers μM	10.9	3.9	8.6	7.75	0.11	25.2
[Pu] μM	55.7	23.1	32.6	62.0	2.0	60
	100 %	41.5 %	58.5 %	100 %	3.2 %	96.8 %

574

575

576 **Table 2** Quantification of the different Pu oxidation states in the *Sporomusa* sp. system determined by
 577 solvent extractions in combination with LSC in the presence of 10 mM Na-pyruvate under steady state
 578 conditions ([Pu]_{initial} 57 ± 1 μM, 0.1 M NaClO₄).

579

	pH 4			pH 6		
	Blank	Supernatant	Biomass	Blank	Supernatant	Biomass
Pu(IV) μM	40.1	20.2	18.3	10.2	2.3	3.8
Pu(VI) μM	-	-	-	-	-	-
Pu(III) μM	0.06	1.83	0.94	31.1	8.01	26.0
Pu(V) μM	-	-	-	-	0.02	-
Pu(IV)-Polymers μM	16.4	6.54	6.76	15.9	6.0	8.9
[Pu] μM	57.6	28.2	29.4	56.5	17.8	38.7
	100%	48.9%	51.0%	100%	31.5%	68.5%

580

581

582

583 **Figure legends**

584

585 **Fig. 1** Eh – pH diagram of Pu calculated for a 0.1 M NaClO₄ solution with 180 μM Pu in the absence of
586 CO₂ at 25 °C. The diagram was constructed using geochemical speciation “Geochemist’s Workbench”®
587 11.0.3 (Bethke 2008) with the NEA Thermochemical Database (Lemire et al. 2001; Guillaumont et al.
588 2003). The diagram includes the measured Eh and pH values from selected experiments at pH 3, 4, 6.1,
589 and 7 (blanks and corresponding cell suspensions).

590

591 **Fig. 2** a and b: Decrease of [²⁴²Pu] in solution at [²⁴²Pu]_{initial}: 188 ± 3 μM in 0.1 M NaClO₄ at pH 4 and 6.1
592 after contact with 0.34 g_{dry weight}/L of *Sporomusa* sp. MT-2.99. The red line represents the best fit of the
593 experimental data. c: Langmuir isotherms obtained in the *Sporomusa* sp. system at pH 4 and 6.1 including
594 the Langmuir absorption isotherm data (a_m maximal Pu loading, b Langmuir constant, R² goodness of fit).

595

596 **Fig. 3** Average ²⁴²Pu oxidation state distributions determined by solvent extraction in 0.1 M NaClO₄
597 without electron donor a) in the supernatant ([dry biomass] 0.34 g/L) at pH 6.1 and b) in the biomass
598 ([dry biomass] 0.34 g/L at pH 4 and 6.1 as well as in the presence of 10 mM Na-pyruvate: c) in the
599 supernatant ([dry biomass] 0.34 g/L at pH 6.1) and d) in the biomass at pH 4 and pH 6.1.

600

601 **Fig. 4** Absorption spectra of Pu ([²⁴²Pu]_{initial} = 450 ± 20 μM) in 0.1 M NaClO₄ at pH 6.1: a) wavelength
602 range of Pu(VI): the supernatants after different contact times with 0.34 g_{dry weight}/L of *Sporomusa* sp. after
603 separating the cells by centrifugation (left) and the blanks (right); b) wavelength range of Pu(V): the
604 supernatants.

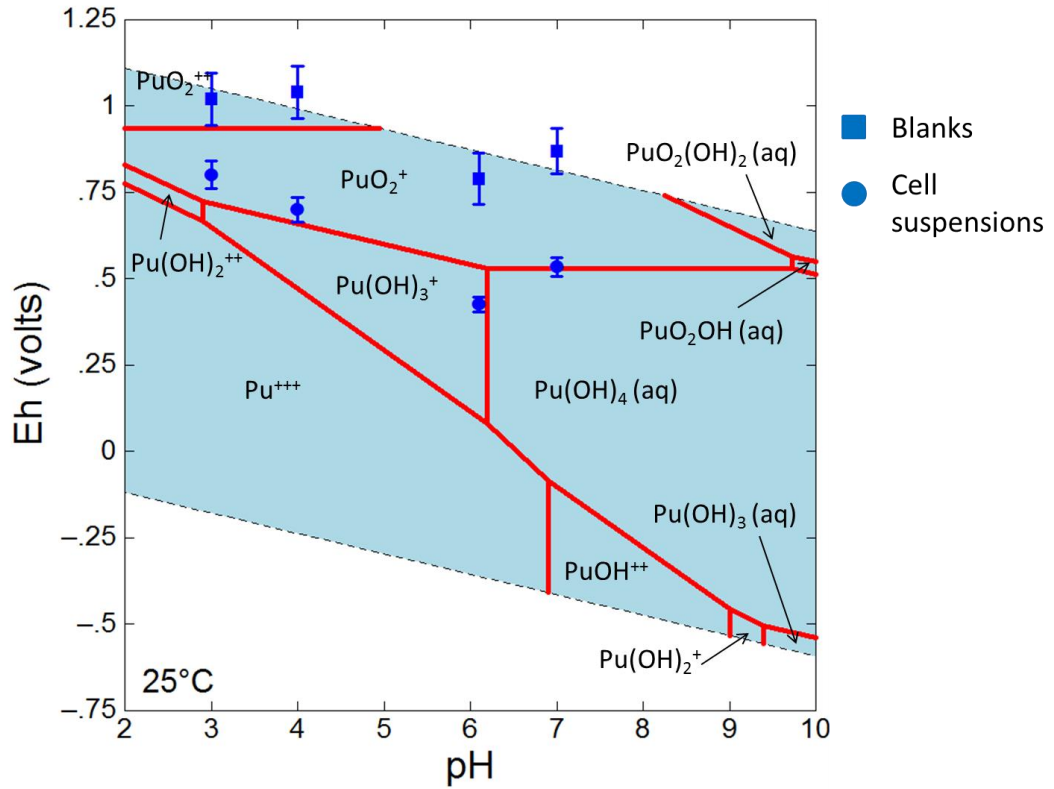
605

606 **Fig. 5** Illustration of the main processes describing the complex interaction of Pu with *Sporomusa* sp.
607 MT-2.99 cells.

608

609

610



611

612

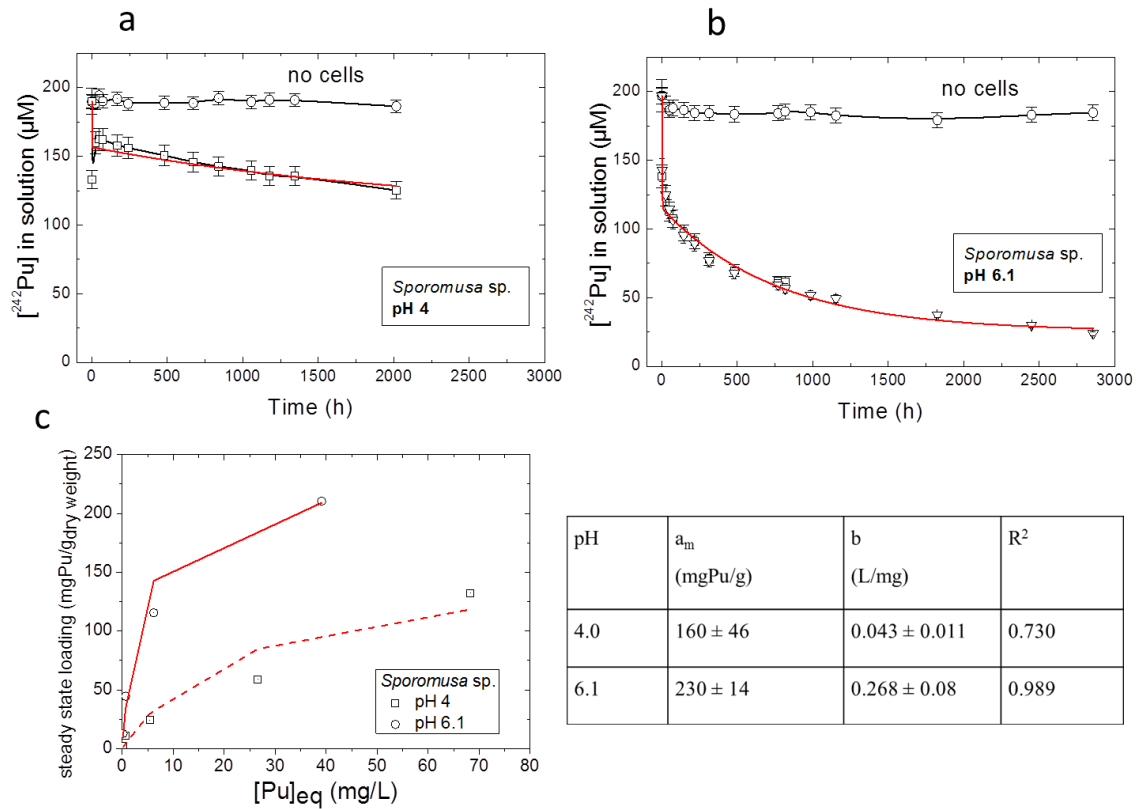
613 **Fig. 1** Eh – pH diagram of Pu calculated for a 0.1 M NaClO₄ solution with 180 μM Pu in the absence of
 614 CO₂ at 25 °C. The diagram was constructed using geochemical speciation “Geochemist’s Workbench”[®]
 615 11.0.3 (Bethke 2008) with the NEA Thermochemical Database (Lemire et al. 2001; Guillaumont et al.
 616 2003). The diagram includes the measured Eh and pH values from selected experiments at pH 3, 4, 6.1,
 617 and 7 (blanks and corresponding cell suspensions).

618

619

620

621



622

623

624 **Fig. 2** a and b: Decrease of $[^{242}\text{Pu}]$ in solution at $[^{242}\text{Pu}]_{\text{initial}}$: $188 \pm 3 \mu\text{M}$ in 0.1 M NaClO_4 at pH 4 and 6.1

625 after contact with $0.34 \text{ g}_{\text{dry weight}}/\text{L}$ of *Sporomusa* sp. MT-2.99. The red line represents the best fit of the

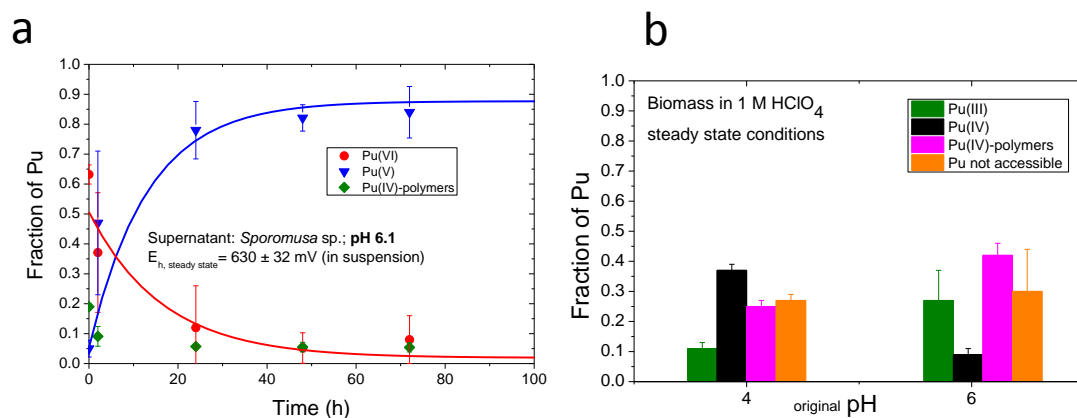
626 experimental data. c: Langmuir isotherms obtained in the *Sporomusa* sp. system at pH 4 and 6.1 including

627 the Langmuir absorption isotherm data (a_m maximal Pu loading, b Langmuir constant, R^2 goodness of fit).

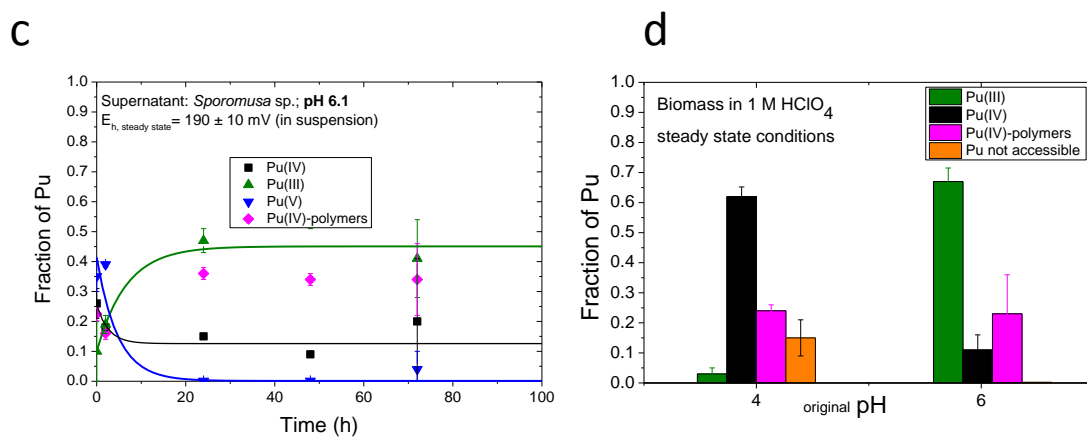
628

629

Without electron donor; $[^{242}\text{Pu}]_{\text{initial}}: 450 \pm 20 \mu\text{M}$



With electron donor; $[^{242}\text{Pu}]_{\text{initial}}: 57 \pm 2 \mu\text{M}$



630

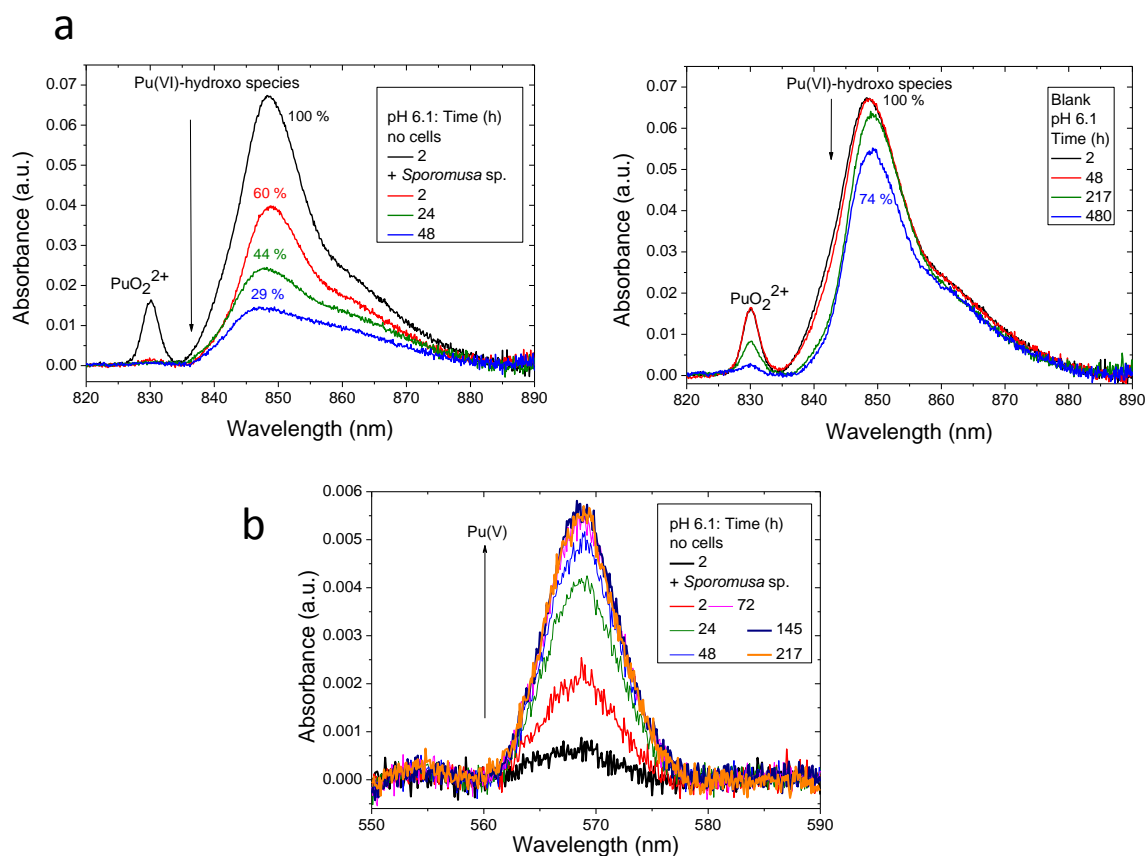
631 **Fig. 3** Average ^{242}Pu oxidation state distributions determined by solvent extraction in 0.1 M NaClO_4

632 without electron donor a) in the supernatant ([dry biomass] 0.34 g/L) at pH 6.1 and b) in the biomass

633 ([dry biomass] 0.34 g/L at pH 4 and 6.1 as well as in the presence of 10 mM Na-pyruvate: c) in the

634 supernatant ([dry biomass] 0.34 g/L at pH 6.1) and d) in the biomass at pH 4 and pH 6.1.

635



636

637

638 **Fig. 4** Absorption spectra of Pu ($[^{242}\text{Pu}]_{\text{initial}} = 450 \pm 20 \mu\text{M}$) in 0.1 M NaClO_4 at pH 6.1: a) wavelength

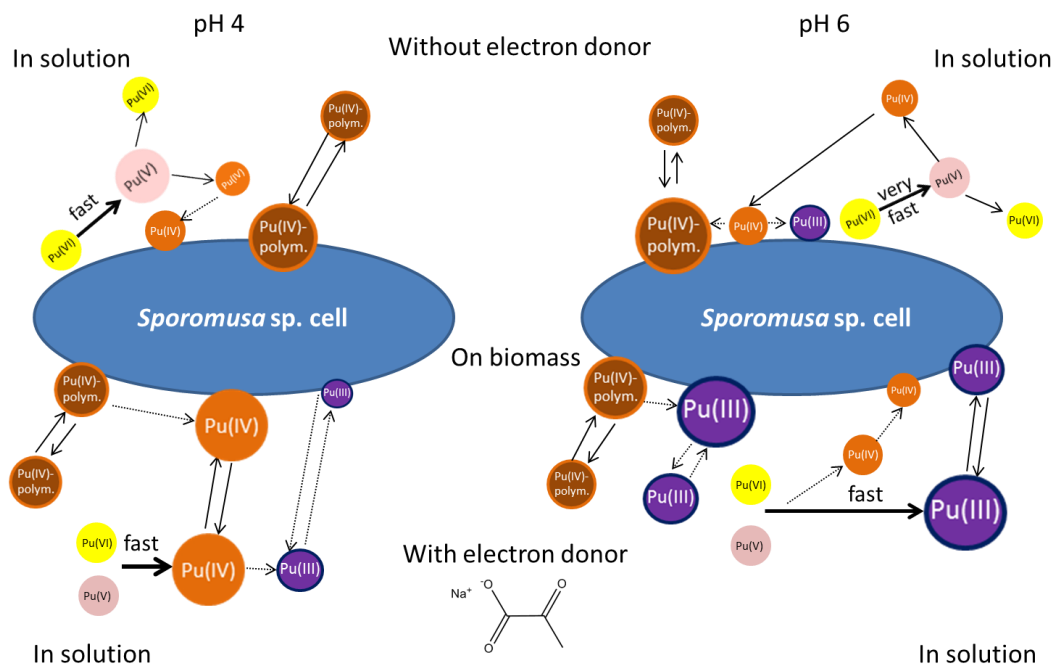
639 range of Pu(VI): the supernatants after different contact times with 0.34 $\text{g}_{\text{dry weight}}/\text{L}$ of *Sporomusa* sp. after

640 separating the cells by centrifugation (left) and the blanks (right); b) wavelength range of Pu(V): the

641 supernatants.

642

643



644

645

646 **Fig. 5** Illustration of the main processes describing the complex interaction of Pu with *Sporomusa sp.*

647 MT-2.99 cells.

648

649

650